Observation of Frequency-Locked Coherent Terahertz Smith-Purcell Radiation

S. E. Korbly, A. S. Kesar, J. R. Sirigiri, and R. J. Temkin

Plasma Science and Fusion Center, Massachusetts Institute of Technology, 167 Albany Street, Cambridge, Massachusetts 02139, USA

(Received 22 September 2004; published 11 February 2005)

We report the observation of enhanced coherent Smith-Purcell radiation (SPR) at terahertz (THz) frequencies from a train of picosecond bunches of 15 MeV electrons passing above a grating. SPR is more intense than other sources, such as transition radiation, by a factor of N_g, the number of grating periods. For electron bunches that are short compared with the radiation wavelength, coherent emission occurs, enhanced by a factor of N_e, the number of electrons in the bunch. The electron beam consists of a train of N_b bunches, giving an energy density spectrum restricted to harmonics of the 17 GHz bunch train frequency, with an increased energy density at these frequencies by a factor of N_b. We report the first observation of SPR displaying all three of these enhancements, $N_g N_e N_b$. This powerful SPR THz radiation can be detected with a high signal to noise ratio by a heterodyne receiver.

DOI: 10.1103/PhysRevLett.94.054803 PACS numbers: 41.60.–m, 07.57.Hm, 29.27.Fh, 52.70.Kz

Electron bunches of subpicosecond duration can be utilized to generate high power, coherent, THz radiation. Recent examples of powerful THz radiation include generation via transition radiation (TR) [1] and synchrotron radiation (SR) [2,3]. This Letter demonstrates a simple method to generate powerful THz radiation by observing Smith-Purcell radiation (SPR) that is enhanced by the number of electrons in a bunch, the number of bunches in a train, and the number of grating periods. SPR, which occurs when a charged particle passes over a periodic structure, was first observed in 1953 [4]. The dispersion relation of the Smith-Purcell radiation is

$$\lambda = \frac{l}{n}\left(\frac{1}{\beta} - \cos\theta\right), \tag{1}$$

where λ is the wavelength of the radiation, n is the order of the radiation, l is the grating period, β is the ratio of the electron velocity to the speed of light, and θ is the observation angle as shown in Fig. 1. A SPR source is higher in intensity by the number of grating periods, N_g, which is typically on the order of 10 to 100, because the bunch radiates at each period of the grating. Moreover, the frequencies are dispersed in angle (θ) according to the resonance condition, Eq. (1), whereas in SR and TR all wavelengths are emitted in a narrow cone for relativistic beams.

For one electron the radiated energy density per unit frequency of the nth order of SPR can be written as [5]

$$\frac{dI_n}{d\omega} = \frac{e^2 N_g l}{8\pi^2 \epsilon_0 c^2}\omega \sin^2\theta \int |R_n|^2 \exp\left[-\frac{x_0}{\lambda_e}\right]\sin^2(\phi)\, d\phi, \tag{2}$$

where x_0 is the height of the electron above the grating, ϕ is the azimuthal angle, $|R_n|^2$ is a grating efficiency factor which is a function of the grating profile, wavelength, and order of radiation [6], and λ_e is the "evanescent wavelength" defined as

$$\lambda_e = \lambda \frac{\beta\gamma}{4\pi\sqrt{1 + \beta^2\gamma^2 \sin^2\theta \sin^2\phi}} \tag{3}$$

with γ the Lorentz factor $(1 - \beta^2)^{-1/2}$.

For N_e electrons in a bunch, coherent radiation is produced for wavelengths longer than the bunch length [7,8]. The total radiated intensity becomes

$$\left(\frac{dI_n}{d\omega}\right)_{N_e} = \left(\frac{dI_n}{d\omega}\right)[N_e S_{\text{inc}} + N_e^2 S_{\text{coh}}(\omega)], \tag{4}$$

where $(dI_n/d\omega)$ is given by Eq. (2). Consider the electron bunch distribution functions to be three independent functions, one for each dimension, $X(x)$, $Y(y)$, $Z(z)$. The incoherent form factor is

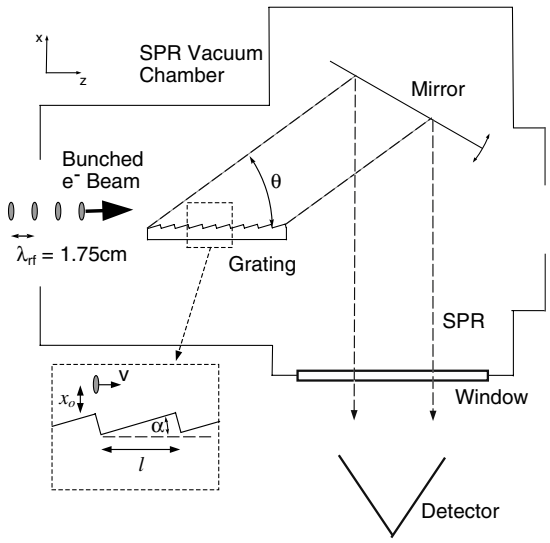

FIG. 1. SPR experimental setup. The train of bunched electrons is traveling along the z direction above a metallic echelle grating. The diffracted radiation is measured by a detector located outside of the vacuum chamber.

$$S_{\mathrm{inc}} = \int_h^\infty dx X(x) e^{-x/\lambda_e}, \tag{5}$$

where h is the maximum height of the grating. The coherent form factor is

$$S_{\mathrm{coh}} = \left| \int_h^\infty dx X(x) e^{-x/2\lambda_e} \tilde{Y}(k_y) \tilde{Z}(\omega) \right|^2, \tag{6}$$

where $\tilde{Y}$ and $\tilde{Z}$ are the Fourier transforms of the bunch distribution functions. The main contribution to the coherence term comes from the longitudinal distribution, $\tilde{Z}(\omega)$, which decays exponentially for wavelengths shorter than the bunch length. Note that in Eq. (4) the second term is about N_e larger than the first term, leading to the enhancement by N_e.

For a train of N_b bunches the total radiated energy density can be written as

$$\left(\frac{dI_n}{d\omega}\right)_{\mathrm{total}} = \left(\frac{dI_n}{d\omega}\right)_{N_e} \left| \sum_{m=1}^{N_b} \exp[i2\pi m \lambda_{\mathrm{rf}}/\lambda] \right|^2 \tag{7a}$$

$$= \left(\frac{dI_n}{d\omega}\right)_{N_e} \left[\frac{\sin(\pi N_b \lambda_{\mathrm{rf}}/\lambda)}{\sin(\pi \lambda_{\mathrm{rf}}/\lambda)} \right]^2, \tag{7b}$$

where λ_{rf} is the distance between bunches, i.e., the rf wavelength. The intensity given by Eq. (7b) has an amplitude of N_b^2 and a bandwidth of N_b^{-1} at the harmonics of the rf frequency. Measurement of this frequency-locked radiation with a coherent measurement system allows a further enhancement of N_b compared to an incoherent detection system. In the present experiment we have measured the SPR with both an incoherent detector, namely, a bolometer, and a coherent detector, namely, a heterodyne receiver, and the results are presented and compared.

The electron bunches are produced by a linear accelerator (linac), built by Haimson Research Corporation (HRC), which consists of a 550 kV electron gun, a chopper prebuncher, and three lens injector, and a quasiconstant gradient accelerating structure consisting of 94 cavities that operate in the $2\pi/3$ mode [9]. The linac is powered by the HRC relativistic klystron [10,11] which was typically operated at 15 MW of rf power at 17.140 GHz in ~100 ns pulses (flattop). The measurements described here were performed with a train of 9 pC, 1 ps electron bunches at a beam energy of 15 MeV with an average current of 0.15 A. The linac has a fill time of 60 ns so the beam is steady state for ~40 ns. The electron beam was approximately 1 mm in diameter with an emittance of 3π mm mrad and the beam centroid height above the grating was set to 0.75 mm.

A theoretical comparison of the radiated energy densities for the MIT electron beam for SPR, SR [12], and TR [13] is shown in Fig. 2. For the SPR calculation the grating consists of ten periods, having 1 cm periodicity and 10° blaze angle (α in Fig. 1). For the SR calculation the bending magnet (90°) radius is assumed to be 1 m and for the TR calculation the foil is considered to be infinite in width. For the SR, TR, and SPR calculations a train of 1500 bunches and measurement using an incoherent detector are assumed. Figure 2 shows the enhancement of the SPR by about N_g, the number of grating periods, which is 10 in this experiment. The second SPR curve, which is labeled FL-SPR, for frequency-locked SPR, includes the effect of coherent detection of the radiation from a train of 1500 bunches. The energy density for FL-SPR is 4 orders of magnitude greater than the SR. The emission in the case of FL-SPR is at discrete frequencies, shown by dots in Fig. 2, and explained further in Figs. 4 and 5 below.

The SPR vacuum chamber shown in Fig. 1 houses the grating, a mirror, and a window and is located 3 m downstream from the exit of the linac. A toroidal focusing lens is located 2 m upstream from the grating, allowing the beam to be focused to an emittance limited spot size of 1.0 mm. The grating, made from oxygen-free high conductivity (OFHC) copper, is an echelle grating with a period of 10 mm with an overall length of 100 mm and a blaze angle of 10°. The grating parameters were chosen to optimize the SPR for a 1.0 ps bunch via the procedure described in [14]. The radiation is directed out of the vacuum chamber via a flat mirror, made from OFHC copper, of overall length of 12.7 cm, and passes through a 10 cm diameter fused silica window. The grating height can be adjusted with two remote controlled stepper motor feedthroughs allowing both the front and the back of the grating to be moved independently. The mirror angle is adjusted via a remote controlled stepper motor. Two different detectors were used to measure the SPR: an Infrared Laboratories Si bolometer and a double heterodyne frequency measurement system. The sensitivity of the bolometer was measured to be 10 mV/nJ. The bolometer is a thermal detector with a bandwidth from approximately 100 GHz to 5 THz. The bolometer response is assumed to be flat down to

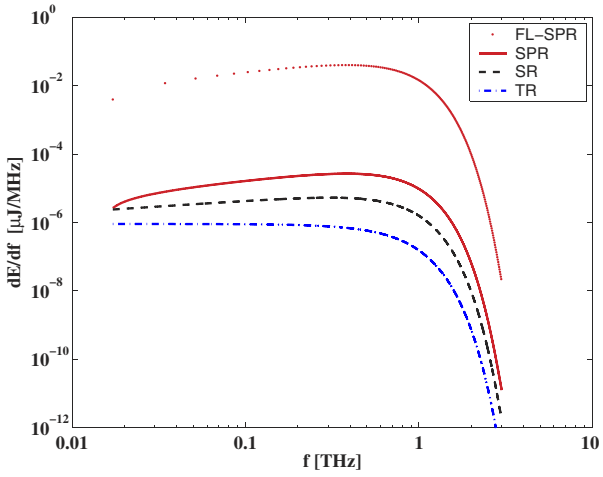

FIG. 2 (color online). Plot of the calculated energy density for various radiation mechanisms using the MIT beam parameters: a 15 MeV beam consisting of 1500 bunches of 6×10^7 electrons (9 pC) with 0.5 ps bunch length.

$\sim$100 GHz before diffraction effects need to be considered. In the double heterodyne system, the first stage is a harmonic mixer capable of operating up to 600 GHz. For this mixer, the rf signal is the SPR, the local oscillator (LO) is a tunable 110–170 GHz backward-wave oscillator, and the intermediate frequency (IF) port, which is followed by an 800 MHz high pass filter and two 19 dB gain low noise amplifiers, produces a signal from 0.8–2.5 GHz. The second stage consists of a 0.3–4.3 GHz mixer, a 2 GHz LO, three low noise amplifiers with 62 dB total gain, and a set of 150 MHz high pass and 550 MHz low pass filters producing an IF of 150–550 MHz. The output of the heterodyne system was analyzed using a fast Fourier transform (FFT) on an 8 GS/s, 500 MHz oscilloscope. Radiation of 200 ns could be analyzed using the heterodyne system. The SPR frequencies were identified by tuning the first LO to find the four peaks on the oscilloscope such that

$$f_{\mathrm{sp}} = j f_{\mathrm{LO1}} \pm f_{\mathrm{LO2}} \pm \Delta, \tag{8}$$

where f_{sp} is the SPR frequency, f_{LO1} is the first LO frequency (tunable from 110–170 GHz), f_{LO2} is the second LO frequency (2 GHz), j is the harmonic of the first LO, and Δ is the frequency separation.

Measurements of the angular distribution of the radiation were made with the Si bolometer as shown in Fig. 3. Also plotted is the theoretical angular distribution of SPR, Eq. (4), for a 15 MeV beam with Gaussian longitudinal and transverse distributions of 1.0 ps FWHM and 1 mm FWHM, respectively. The theoretical distribution of radiation is computed for $\phi = 0$ and the grating efficiency factor, $|R_n|^2$, is computed using an integral equation model [5,15]. Since the form factor, defined in Eq. (6), falls off exponentially when the wavelength is shorter than the bunch length, the fit is most sensitive to the high frequency data. The bolometer is unable to detect the frequency structure described by Eq. (7b) due to the fact that it is a thermal detector with a slow time response and a broad frequency acceptance. The larger error bars at angles $>35°$ are due to the fact that the radiation collection system was unable to collect all the radiation at higher angles due to vacuum chamber geometrical constraints. The dependence of the SPR intensity on beam current was measured, and it scaled quadratically as predicted for coherent SPR. The intensity of the SPR was observed to be proportional to the macrobunch length, in agreement with the dependence of Eq. (7b) on N_b.

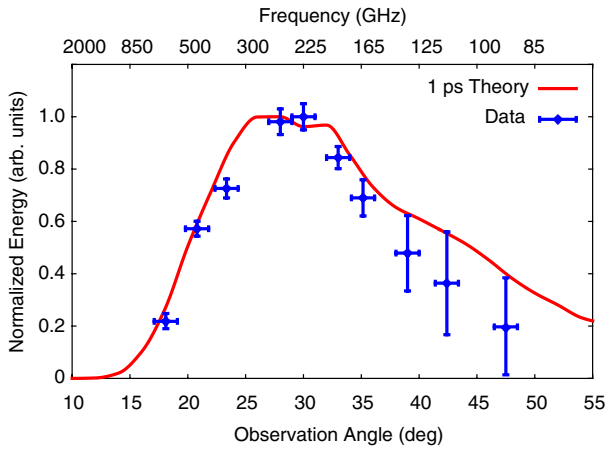

FIG. 3 (color online). Plot of the angular distribution of SPR normalized energy as measured by the Si bolometer. The theoretical curve is shown for a 15 MeV beam with a 1.0 ps FWHM Gaussian longitudinal distribution and a 1 mm FWHM Gaussian transverse distribution.

A detailed search in frequency space using the double heterodyne system indicated frequency-locked SPR, with frequencies only at integer multiples of the accelerator frequency as shown in Fig. 4. Each peak had a width of $\sim$25 MHz, corresponding to a linewidth of 0.01%, due to the 40 ns of steady state electron beam. Frequencies missing in Fig. 4 could not be observed with the available double heterodyne receiver because the required LO frequencies are outside the 110–170 GHz range. The slope of the fitted line matches the accelerator frequency to within 1 MHz. Small changes of order 5 to 10 MHz in the 17.14 GHz accelerator frequency resulted in comparable and reproducible changes in the SPR radiation frequencies. Figure 5 compares the measured power of the FFT of the IF for a 240 GHz (14th harmonic) peak to theory. The theoretical curve, Eq. (7b), for $N_b = 550$ matches the data extremely well, even showing the 2nd maxima in detail.

We have observed the first frequency locking of coherent SPR using a double heterodyne frequency measurement system. The use of a coherent detection system enables us to measure the total enhancement of the intensity of $N_g N_e N_b$. Moreover, the use of a heterodyne receiver frequency detection system allows a high signal to noise ratio using a room temperature detector and could lead to advances in THz spectroscopy. Additionally, we have demonstrated the generation of high intensity THz SPR from a

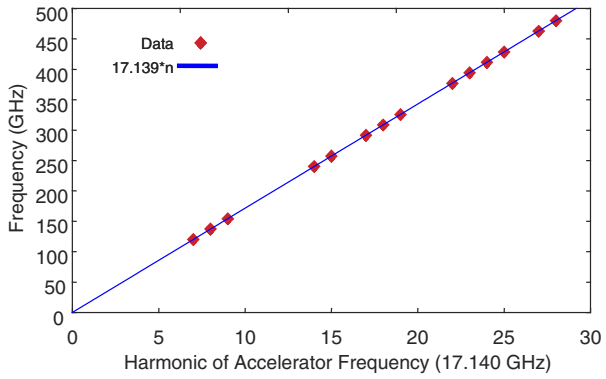

FIG. 4 (color online). Plot of the frequency spectrum of SPR as measured by the double heterodyne receiver. The accelerator rf frequency was 17.140 GHz.

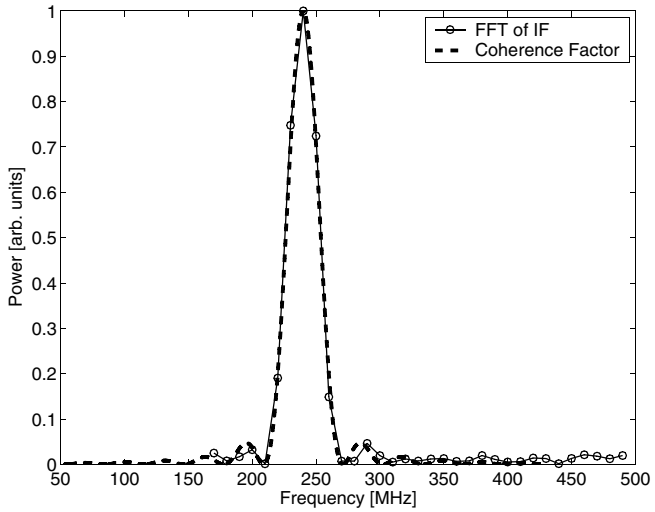

FIG. 5. Comparison of the measured power in the FFT of the IF signal from the SPR as measured by the double heterodyne receiver and the theoretical prediction. The peak corresponds to a radiation frequency of 240 GHz (14th harmonic) and has 28 MHz FWHM. The theoretical curve is calculated using $N_b = 550$. Experimental data below 170 MHz have been omitted because of the low frequency noise in the receiver which is blocked by the low pass filter.

compact rf accelerator. The SPR exhibits relatively flat power levels for frequencies over a wide frequency range. A specific frequency can be chosen by restricting the collection optics to a small angular range. Frequency step tuning could then be obtained by rotating the mirror (see Fig. 1). This is an advantage over SR and TR which require a dispersive element (grating or interferometer) for wavelength selectivity. Coherent SPR can produce several orders of magnitude higher energy and power levels than coherent SR and should be considered for THz radiation production at light sources. The measurement of the angular distribution of the radiation determined the longitudinal bunch length to be 1.0 ± 0.1 ps. The use of SPR as a bunch length diagnostic has the advantage that it is a nondestructive technique and is important for FEL's and next generation linear colliders. This measured bunch length agrees with an independent circularly polarized deflection measurement [16].

This work was supported by the Department of Energy, Division of High Energy Physics, Contract No. DE-FG02-91ER40648. The authors thank Dr. Jake Haimson and the Haimson Research Corporation for help and advice in running the accelerator, Dr. Hayden Brownell for his advice on the SPR experimental setup, and Ivan Mastovsky, Roark Marsh, and Dr. Michael Shapiro for their help in running the experiments.

[1] W. P. Leemans *et al.*, Phys. Rev. Lett. **91**, 074802 (2003).
[2] M. Abo-Bakr *et al.*, Phys. Rev. Lett. **90**, 094801 (2003).
[3] G. L. Carr *et al.*, Nature (London) **420**, 153 (2002).
[4] S. Smith and E. Purcell, Phys. Rev. **92**, 1069 (1953).
[5] P. M. van den Berg, J. Opt. Soc. Am. **63**, 1588 (1973).
[6] O. Haeberle *et al.*, Phys. Rev. E **49**, 3340 (1994).
[7] S. Nodvick and D. S. Saxon, Phys. Rev. **96**, 180 (1954).
[8] C. J. Hirschmugl *et al.*, Phys. Rev. A **44**, 1316 (1991).
[9] J. Haimson and B. Mecklenburg, in *Proceedings of the 1995 Particle Accelerator Conference* (IEEE, Piscataway, NJ, 1996), Cat. No. 95CH35843, p. 755.
[10] J. Haimson, IEEE Trans. Nucl. Sci. **3**, 996 (1965).
[11] J. Haimson *et al.*, in *Proceedings of the 1999 Conference on High Energy Density Microwaves*, AIP Conf. Proc. No. 474 (AIP, New York, 1999), p. 137.
[12] H. Wiedemann, *Particle Accelerator Physics II* (Springer, New York, 1999).
[13] V. L. Ginzburg and V. N. Tsytovich, *Transition Radiation and Transition Scattering* (Adam Hilger, New York, 1990).
[14] S. Trotz *et al.*, Phys. Rev. E **61**, 7057 (2000).
[15] A. S. Kesar, M. Hess, S. E. Korbly, and R. J. Temkin, Phys. Rev. E **71**, 016501 (2005).
[16] J. Haimson, in *Proceedings of the 2004 Advanced Accelerator Concepts Conference*, AIP Conf. Proc. 737 (AIP, New York, 2004), pp. 95–108.